FRAGMENTS OF OENOCHOE GV132-01/US26-OBJ.10 - TIN BRONZE - ROMAN TIMES - SWITZERLAND

Artefact name	Fragments of oenochoe GV132-01/US26-obj.10
Authors	Christian. Degrigny (HE-Arc CR, Neuchâtel, Neuchâtel, Switzerland) & S. Gillioz (HE-Arc CR, Neuchâtel, Neuchâtel, Switzerland) & Valentin. Boissonnas (HE-Arc CR, Neuchâtel, Neuchâtel, Switzerland)
Url	/artefacts/460/

The object

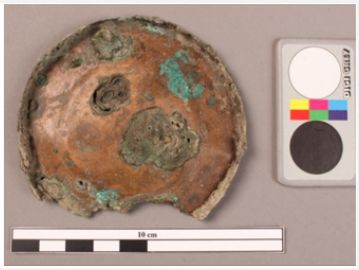

Credit HE-Arc CR, S.Gillioz.

Fig. 1: Oenochoe, belly / neck of the vessel with its base. Only the base is considered in the present file,

Description and visual observation

Description of the artefact	Base of an oenochoe (Fig. 1). Dimensions: L = 82 mm; W = 74 (after degradation) ; T =6,5 mm; WT = 30,9 g.
Type of artefact	Oenochoe, vessel
Origin	Place Simon-Goulart, Genève, Geneva, Switzerland
Recovering date	Excavation 2012
Chronology category	Roman Times
chronology tpq	20 B.C.
chronology taq	50 A.D.
Chronology comment	
Burial conditions / environment	Soil
Artefact location	Service cantonal d'archéologie, Genève, Geneva
Owner	Service cantonal d'archéologie, Genève, Geneva
Inv. number	GV132-01/US26-obj.10
Recorded conservation data	Not conserved

Complementary information

This work is licensed under CC BY-NC-ND 4.0

Nothing to report.

Study area(s)

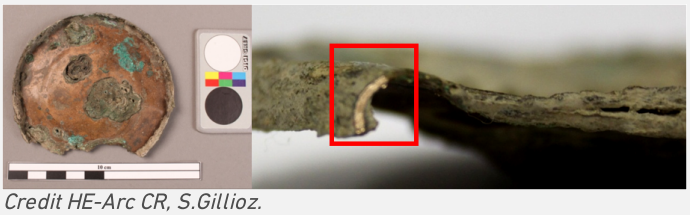

Credit HE-Arc CR, S.Gillioz.

Fig. 2: Location of sampling area,

Binocular observation and representation of the corrosion structure

The schematic representation below gives an overview of the corrosion layers encountered on the oenochoe base from visual macroscopic observation.

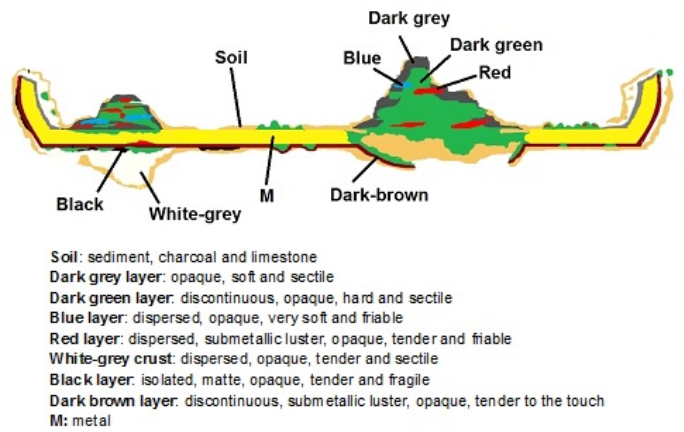

Credit HE-Arc CR, S.Gillioz.

Fig. 3: Stratigraphic representation of the oenochoe base in cross-section by macroscopic observation,

MiCorr stratigraphy(ies) – Bi

Sample(s)

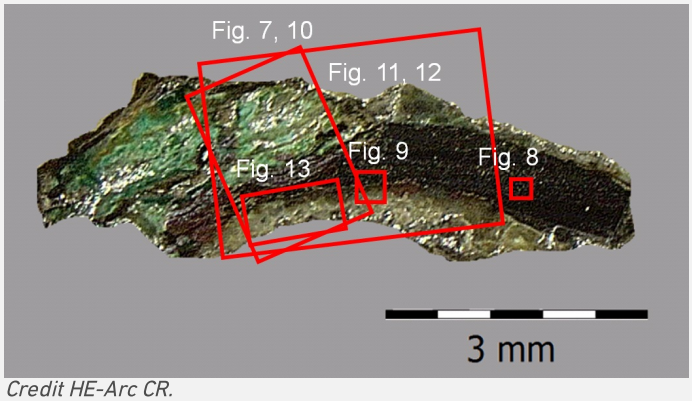

Credit HE-Arc CR.

Fig. 4: Micrograph of the cross-section showing the location of Figs. 7 to 13,

This work is licensed under CC BY-NC-ND 4.0

Description of sample	The sample was cut from the edge shown in Fig. 2. Its dimensions are L = 6.5 mm, W = 1.5 mm. The sample contains some remaining metal covered with a crust and a voluminous pustule corrosion (Fig. 4).
Alloy	Tin Bronze
Technology	Cold worked with repeated annealing and final cold working
Lab number of sample	HECR 1455 – S2
Sample location	HE-Arc CR, Neuchâtel, Neuchâtel
Responsible institution	Musée cantonal d'archéologie et d'histoire, Lausanne, Vaud
Date and aim of sampling	2013, metallography and chemical analyses

Complementary information

Nothing to report.

Analyses and results

Analyses performed:
Metallography (etched with ferric chloride reagent), SEM-EDS.

Non invasive analysis

Metal

The remaining metal is a tin bronze (Table 1). The etched metal shows a structure of polygonal grains with twinned and strain lines (Fig.8).

Elements	Cu	Sn
mass%	91	9

Table 1: Chemical composition of the metal. Method of analysis: SEM-EDS, Lab of Electronic Microscopy and Microanalysis, IMA (Néode), HEI Arc.

Fig. 7: SEM image of the metal sample from Fig.4 (rotated 30°), BSE-mode,

This work is licensed under CC BY-NC-ND 4.0

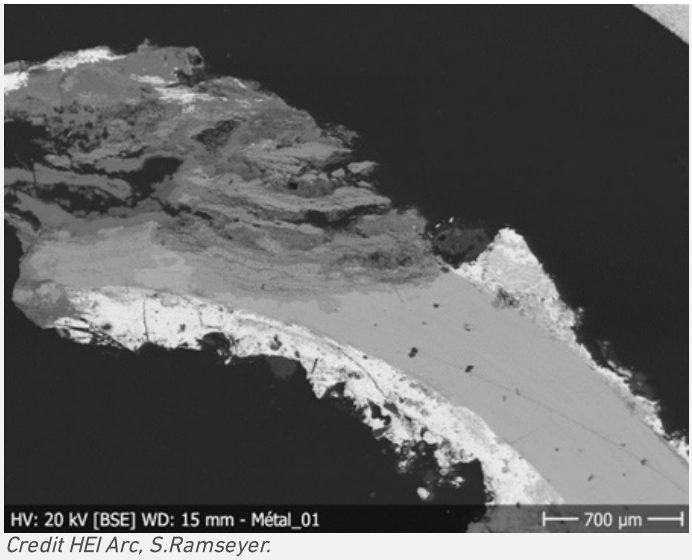

Credit HEI Arc, S.Ramseyer.

Credit HE-Arc CR.

Fig. 8: Micrograph of the metal sample from Fig. 4, etched, bright field, 50x. Polygonal and twinned grains with strain lines are observed. The dotted surface is the result of over-etching,

Microstructure	Polygonal grains with twinned and strain lines
First metal element	Cu
Other metal elements	Sn

Complementary information

Nothing to report.

Corrosion layers

Intergranular corrosion is observed on the edges of the remaining metal (Fig. 9).The sample shows two forms of corrosion: multi-layered pustule corrosion at the left extremity of the sample (Fig. 10, area 1) and a corrosion crust covering the metal (Fig.10, area 2). The multi-layered pustule corrosion has an average thickness of about 1.1 mm (L) and 0.79 mm (W) (Fig.11). It is composed of a sandwich of 7 corrosion products, mainly green, grey, red and blue in dark field. Microscopic observation allows us to highlight new corrosion products that were not detected during the first visual examination (Fig. 11):

CP1. Light grey layer, containing mainly Sn, O, some Fe, P and a small amount of Pb combined with dark green layer, containing mainly Cu, O and P (Fig. 12, Fig. 5 and table 2)

CP2. Blue layer, containing mainly Cu, Cl (Fig. 12, Fig. 5 and table 2)

CP3. Red layer, containing mainly Cu and O combined with black layer containing mainly Sn and O (Fig. 12, Fig. 5 and table 2)

CP4. Brown layer containing mainly Cu, Sn and O (Fig. 12, Fig. 5 and table 2)

CP5. Dark grey layer containing mainly Cu, Sn and O (Fig. 12, Fig. 5 and table 2)

This work is licensed under CC BY-NC-ND 4.0

Superior markers such as contextual Fe and P are present in several layers. Their penetration illustrates the cracking of the primary corrosion layer during the formation of the pustule. The P-enrichment in some corrosion layers may be due to an environment rich in organic material (for example bones). The multi-layered pustule corrosion type has developed similarly to the process presented by Formigli (1975, p.53) and Scott (2002, p.337).

The corrosion crust on the metal has an average thickness of about 70 µm (Fig. 13). It consists of two sub-layers. The inner corrosion layer (CP2) is thin and dark brown in dark field or light grey in bright field. It has penetrated into the metal structure in some areas (Fig. 9). In dark field, the outer corrosion layer (CP1) is constituted of a heterogeneous light grey corrosion crust (Fig.13). The inner brown corrosion layer is enriched in Sn and O but also contains P, while the outer light grey corrosion layer is mainly composed of Pb and O but also contains P and Fe (Fig. 12). The outer light grey layer is probably due to the presence of a soft solder used to assemble the base to the body.

Elements	Cu	Sn	O	P	Fe	Pb	Cl
Grey layer	nd	+++	++	++	++	+	nd
Dark green layer	++	nd	+++	+++	+	+	+
Blue layer	+++	nd	+	nd	nd	nd	+++
Red layer	+++	nd	++	nd	+	nd	nd
Black layer	nd	+++	+++	+	+	+	nd
Brown layer	++	++	++	nd	nd	nd	nd
Dark grey layer	++	++	++	nd	nd	nd	nd
Light grey layer (crust)	nd	nd	++	+	+	+++	nd
Dark brown layer (crust)	nd	+++	++	+	+	+	nd

Table 2: Chemical composition of the multi-layered pustule corrosion from Figs. 10, 11 and 12 in dark field. SEM-EDS, Lab of Electronic Microscopy and Microanalysis, IMA (Néode) (+++: high concentration, ++ medium concentration, + low concentration, nd: not-detected).

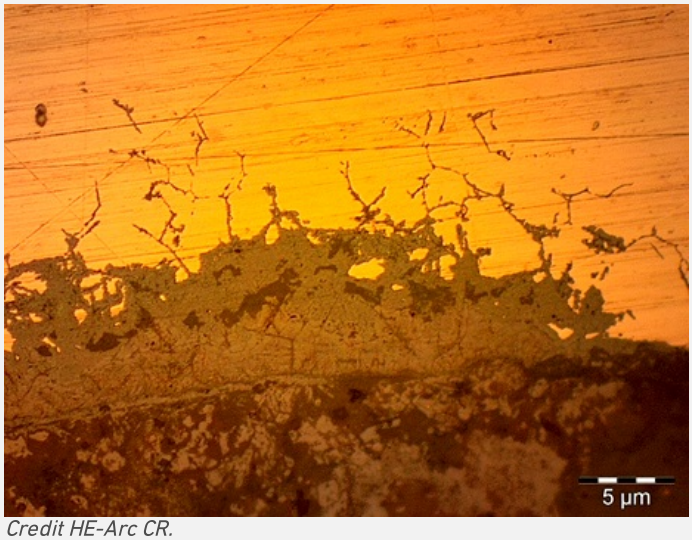

Credit HE-Arc CR.

Fig. 9: Micrograph of the metal sample from Fig. 4, unetched, bright field, 50x. The grain boundaries are revealed by the intergranular corrosion,

Fig. 10: Micrograph of the metal sample (same as Fig. 7, 30° rotated), unetched, dark field, showing the location of the multi-layered pustule corrosion (area 1 to compare to Fig. 5) and the corrosion crust (area 2 to compare to Fig. 6). The mapped area (Fig. 12) is marked by a red rectangle,

This work is licensed under CC BY-NC-ND 4.0

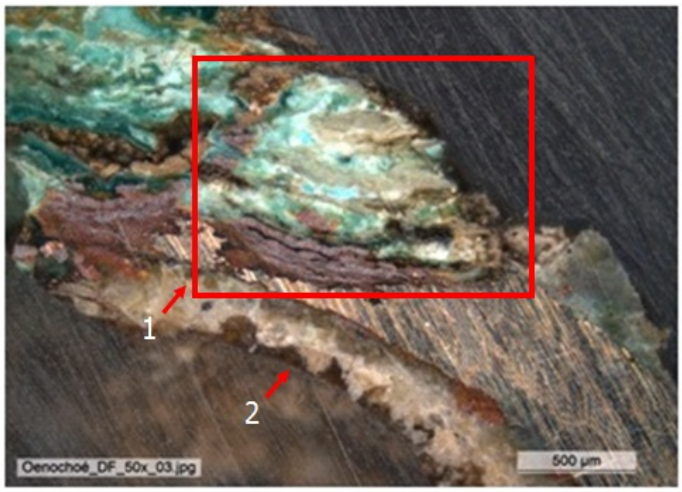

Credit HE-Arc CR.

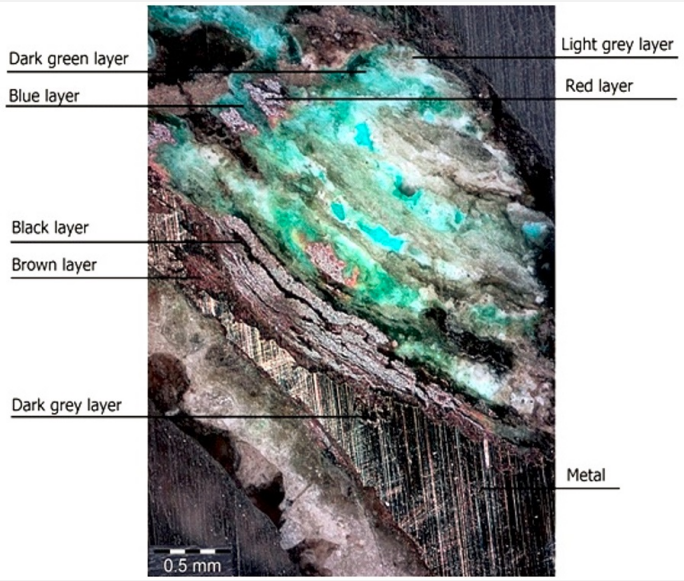

Credit HE-Arc CR.

Fig. 11: Micrograph of the metal sample from Fig. 10 (area 1, 60° rotated) and corresponding to the stratigraphy of Fig. 5, unetched, dark field,

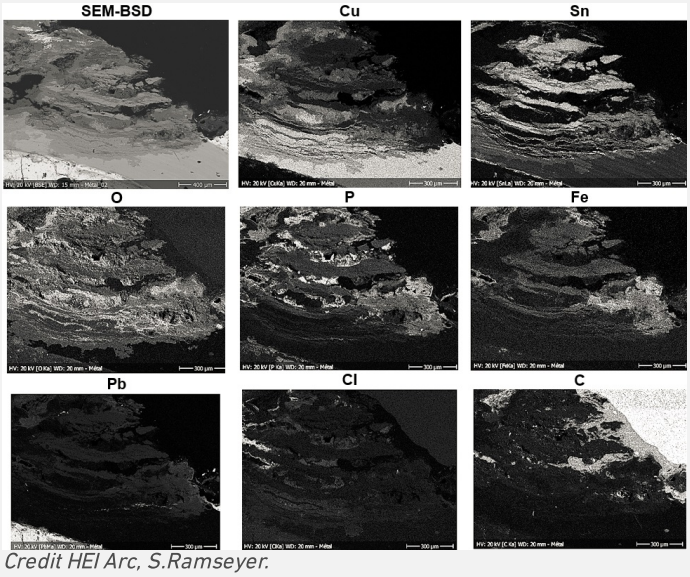

Credit HEI Arc, S.Ramseyer.

Fig. 12: SEM image, SE-mode, and elemental chemical distribution of the selected area of Fig. 11. Method of examination: SEM-EDS, Lab of Electronic Microscopy and Microanalysis, IMA (Néode), HEI Arc,

Fig. 13: Micrograph of the metal sample (area 2) from Fig.10 (detail) and corresponding to the stratigraphy of Fig. 6, dark field,

This work is licensed under CC BY-NC-ND 4.0

Credit HE-Arc CR.

Corrosion form	Multiform (warty - uniform) - pitting
Corrosion type	Both Formigli (pustules) and type I (Robbiola) otherwise

Complementary information

Nothing to report.

MiCorr stratigraphy(ies) – CS

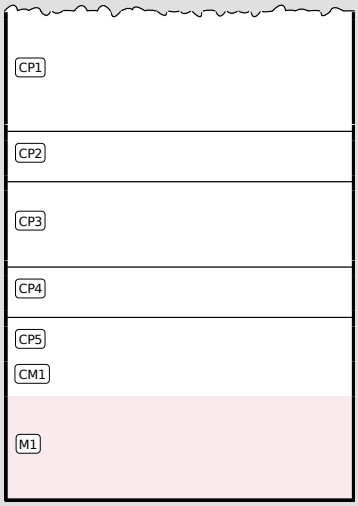

Fig. 5: Stratigraphic representation of the object in cross-section using the MiCorr application. The characteristics of the strata are only accessible by clicking on the drawing that redirects you to the search tool by stratigraphy representation. This representation can be compared to Fig. 11, Credit HE-Arc CR, C.Degrigny.

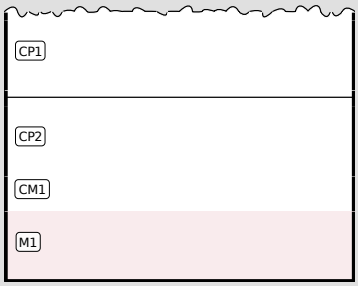

Fig. 6: Stratigraphic representation of the object in cross-section using the MiCorr application. The characteristics of the strata are only accessible by clicking on the drawing that redirects you to the search tool by stratigraphy representation. This presentation can be compared to Fig. 13, Credit HE-Arc CR, C.Degrigny.

Synthesis of the binocular / cross-section examination of the corrosion structure

Based on the analyses carried out, the stratigraphy of the multi-layered pustule has been corrected. The addition of "e" and "i" within the coding refers to the location of the strata which are either internal ("i") or in contact with the atmosphere ("e").

Fig. 14: Improved stratigraphic representation of the multi-layered pustule form on the oenochoe from visual observations and analyses,

This work is licensed under CC BY-NC-ND 4.0

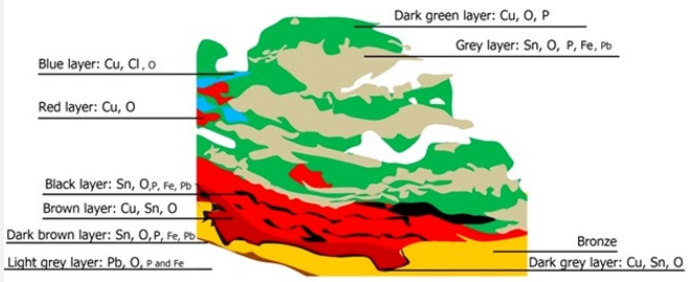

Dark green layer (CP1e)	Cu, O, P
Grey layer (CP2e)	Sn, O, P
Blue layer (CP3i)	Cu, Cl, O
Red layer (CP4i)	Cu, O
Black layer (CP5i)	Sn, O
Brown layer (CP6i)	Cu, Sn, O

Credit HE-Arc CR, S.Gillioz

Conclusion

The metal of the oenochoe's base is a tin bronze. The polygonal and twinned grains with strain lines show that the base has been repeatedly cold worked and annealed with a final cold work. The metal is either well preserved or heavily corroded with the formation of pustules that go through the whole thickness of the metal. The limit of the original surface corresponds to the top surface of the dark brown layer. In the presence of a pustule it is highly deformed but discernible by the tin enriched surface. The corrosion is multiform. The well preserved and only lightly corroded areas are of Robbiola type 1 (Robbiola et al. 1998), the pustules however are of the Formigli type (Formigli 1975).

References

References on object and sample

Reference object

1. Gillioz S. (2012) Oenochoé GV132-01/US.26-obj.10, Genève, Place Simon-Goulart, rapport d'intervention. Haute Ecole ARC, Neuchâtel, 2013, non-publié.

Reference sample

2. Gillioz S. (2012) Oenochoé GV132-01/US.26-obj.10, Genève, Place Simon-Goulart, rapport d'intervention. Haute Ecole ARC, Neuchâtel, 2013, non-publié.

References on analytic methods and interpretation

3. Formigli, E. « Die Bildung von Schichtpocken auf antiken Bronzen ». Arbeitsblätter, Heft 1, 1975, p.51 à 74.
4. Robbiola, L., Blengino, J-M., Fiaud, C. (1998) Morphology and mechanisms of formation of natural patinas on archaeological Cu-Sn alloys, Corrosion Science, 40, 12, 2083-2111.
5. Scott, D. A. Copper and bronze in Art, corrosion, colorants, conservation. Getty publications, Los Angeles, 2002.

This work is licensed under CC BY-NC-ND 4.0